TRANSCRIPTIONAL PROFILING OF *MYCOBACTERIUM SMEGMATIS* EXPOSED TO SUBINHIBITORY CONCENTRATIONS OF G4-STABILIZING LIGANDS

Zaychikova MV, Bespiatykh DA, Malakhova MV, Bodoev IN, Vedekhina TS, Veselovsky VA, Klimina KM, Varizhuk AM, Shitikov EA✉

Federal Research and Clinical Center of Physical-Chemical Medicine, Moscow, Russia

The spread of *Mycobacterium tuberculosis* drug resistance accentuates the demand for anti-tuberculosis drugs with a fundamentally new mechanism of action without conferring cross-resistance. G-quadruplexes (G4, non-canonical DNA structures) are plausible new drug targets. Although G4-stabilizing ligands have been shown to inhibit mycobacterial growth, the exact mechanism of their action is uncertain. The aim of this study was to assess a possible correlation between putative G4 elements in a model mycobacterial strain *M. smegmatis* MC2155 and transcriptomic changes under the action of subinhibitory concentrations of G4 ligands BRACO-19 and TMPyP4. We also planned to compare the results with corresponding data previously obtained by us using higher, inhibitory concentrations of these ligands. For BRACO-19, we identified 589 (316↑; 273↓) and 865 (555↑; 310↓) differentially expressed genes at 5 μM and 10 μM, respectively. For TMPyP4, we observed the opposite trend, the number of differentially expressed genes decreased at higher concentration of the ligand: 754 (337↑; 417↓) and 702 (359↑; 343↓) for 2 μM and 4 μM, respectively. Statistical analysis revealed no correlation between ligand-induced transcriptomic changes and genomic localization of the putative quadruplex-forming sequences. At the same time, the data indicate certain functional specificity of the ligand-mediated transcriptomic effects, with TMPyP4 significantly affecting expression levels of transcription factors and arginine biosynthesis genes and BRACO-19 significantly affecting expression levels of iron metabolism and replication and reparation system genes.

Keywords: G-quadruplexes, transcriptomic analysis, *Mycobacterium smegmatis*, *Mycobacterium tuberculosis*, BRACO-19, TMPyP4, antimicrobial therapy

Funding: the study was funded by the Russian Science Foundation, project number 19-75-10109

Author contribution: Zaychikova MV — literature analysis, data analysis and interpretation, manuscript drafting; Bespiatykh DA — literature analysis, data analysis, manuscript drafting; Malakhova MV — research planning and implementation; Bodoev IN — literature analysis, data analysis, manuscript drafting; Vedekhina TS — research implementation, data interpretation; Veselovsky VA — research implementation, data analysis; Klimina KM — research implementation, data analysis and interpretation; Varizhuk AM — research planning and implementation, data interpretation; Shitikov EA — research planning, literature analysis, data analysis, manuscript drafting.

✉ **Correspondence should be addressed:** Egor A. Shitikov
Malaya Pirogovskaya, 1a, Moscow, 119435, Russia; eshitikov@mail.ru

Received: 08.04.2022 **Accepted:** 30.04.2022 **Published online:** 15.05.2022

DOI: 10.24075/brsmu.2022.024

ВЛИЯНИЕ СУБИНГИБИРУЮЩИХ КОНЦЕНТРАЦИЙ G4-СТАБИЛИЗИРУЮЩИХ ЛИГАНДОВ НА ТРАНСКРИПТОМНЫЙ ПРОФИЛЬ *MYCOBACTERIUM SMEGMATIS*

М. В. Зайчикова, Д. А. Беспятых, М. В. Малахова, И. Н. Бодоев, Т. С. Ведехина, В. А. Веселовский, К. М. Климина, А. М. Варижук, Е. А. Шитиков ✉

Федеральный научно-клинический центр физико-химической медицины Федерального медико-биологического агентства, Москва, Россия

В связи с широким распространением лекарственной устойчивости у *Mycobacterium tuberculosis* особое значение приобретает поиск противотуберкулезных препаратов с принципиально новым механизмом действия, исключающим развитие перекрестной устойчивости. В этом отношении определенный интерес представляют G-квадруплексы (G4) — неканонические структуры ДНК, участвующие в регуляции и поддержании стабильности генома. Показано, что G4-стабилизирующие соединения, лиганды, оказывают ингибирующий эффект на рост микроорганизма, но точный механизм их действия неизвестен. Целью исследования было выявить связь между наличием потенциальных G4 в геноме модельного микроорганизма *M. smegmatis* mc2 155 и изменением транскриптомного профиля под действием субингибирующих концентраций лигандов BRACO-19 и TMPyP4, а также провести сравнительный анализ результатов с данными, полученными нами ранее для ингибирующих концентраций указанных лигандов. Под действием BRACO-19 было идентифицировано 589 (316↑; 273↓) и 865 (555↑; 310↓) дифференциально экспрессированных генов, для 5 и 10 мкМ соответственно. Напротив, в случае с TMPyP4 обнаружено снижение числа дифференциально экспрессированных генов с 754 (337↑; 417↓) до 702 (359↑; 343↓) для концентраций 2 и 4 мкМ соответственно. Статистический анализ не выявил связи между изменением уровня экспрессии генов под действием лигандов и наличием потенциальных квадруплекс-формирующих последовательностей, вне зависимости от локализации G4. Тем не менее было установлено, что TMPyP4 вызывает значительные изменения в экспрессии факторов транскрипции и генах биосинтеза аргинина, а BRACO-19 — в генах метаболизма железа, а также в генах систем репликации и репарации.

Ключевые слова: G-квадруплексы, транскриптомный анализ, *Mycobacterium smegmatis*, *Mycobacterium tuberculosis*, BRACO-19, TMPyP4, антимикробная терапия

Финансирование: исследование выполнено за счет гранта Российского научного фонда (проект №19-75-10109).

Вклад авторов: М. В. Зайчикова — анализ литературы, анализ и интерпретация данных, подготовка черновика рукописи; Д. А. Беспятых — анализ литературы, анализ данных, подготовка черновика рукописи; М. В. Малахова — планирование и проведение исследования; И. Н. Бодоев — анализ литературы, анализ данных, подготовка черновика рукописи; Т. С. Ведехина — проведение исследования, интерпретация данных; В. А. Веселовский — проведение исследования, анализ данных; К. М. Климина — проведение исследования, анализ и интерпретация данных; А. М. Варижук — планирование и проведение исследования, интерпретация данных; Е. А. Шитиков — планирование исследования, анализ литературы, анализ данных, подготовка черновика рукописи.

✉ **Для корреспонденции:** Егор Александрович Шитиков
ул. Малая Пироговская, д. 1а, г. Москва, 119435, Россия; eshitikov@mail.ru

Статья получена: 08.04.2022 **Статья принята к печати:** 30.04.2022 **Опубликована онлайн:** 15.05.2022

DOI: 10.24075/vrgmu.2022.024

Tuberculosis, caused by *Mycobacterium tuberculosis* complex, is a global problem for modern healthcare. According to WHO expert estimates, in 2020 the number of deaths caused by the disease increased by 100,000 people compared to 2019 and amounted to 1.3 million. The negative trend is expected to continue in the coming years, reflecting a reduction in funding for tuberculosis diagnostics and treatment amid the overall strain on global healthcare due to the COVID-19 pandemic [1].

Despite the use of anti-tuberculosis therapy, the treatment success rate for drug-resistant cases does not exceed 60%. The ubiquitously emerging resistance of mycobacterial strains to new drugs such as linezolid, bedaquiline, clophosamine, etc. [2] accentuates the demand for new anti-tuberculosis drugs with a fundamentally different mechanism of action, as well as new targets for anti-tuberculosis therapy.

One plausible new target is represented by G-quadruplexes (G4) — non-canonical secondary structures formed by guanine-rich DNA and RNA sequences under physiological conditions. Each structural unit of G4 — G-quartet — consists of four guanine bases. The G-quartets are held together by ϖ-ϖ-stacking interactions and additionally stabilized by metal cations [3].

In eukaryotes, such non-canonical nucleic acid structures are fairly well studied and play an important role in genome stability regulation and maintenance [4]. In the 2000s, putative quadruplex sequences (PQS) were discovered in genomes of many bacteria and archaea, but their functional role requires further investigation [5]. G4 are possibly involved in various aspects of bacterial physiology, including survival in adverse environments, pathogenic bacteria interactions with the host, antigenic variation, etc. [6].

G4 ligands, typically compounds with low-molecular weight, bind the quadruplexes and affect their thermal stability, which may displace or reestablish certain protein factors and enzymes functionally associated with DNA or RNA and ultimately interfere with transcription and translation. The best known G4 ligands include acridine derivative BRACO-19 and cationic porphyrin TMPyP4 (Fig. 1). Potential use of G4-ligands as antimicrobials has been demonstrated for *Vibrio cholerae*, *Klebsiella pneumoniae*, *Streptococcus pneumoniae* and *Mycobacterium tuberculosis* [6].

Tuberculosis mycobacteria, with their high GC content and considerable PQS density, represent a promising target for antimicrobial action of G4-stabilizing ligands. Inhibition of their growth by micromolar concentrations of known G4-ligands c-exNDI-2, BRACO-19 and TMPyP4 has been previously demonstrated. In these experiments, c-exNDI-2 and BRACO-19 exerted stabilizing effects on particular G-quadruplex elements located in promoter regions [7]. Similarly, TMPyP4 exerted a stabilizing effect on quadruplexes located in virulence-associated genes [8].

It should be emphasized that all the aforementioned studies were focused on quadruplex-forming sequences at particular genomic locations; notably, the presence of G4 was invariably associated with inhibited expression of the corresponding gene under the action of ligand. In our previous study, we analyzed the transcriptomic response to inhibitory concentrations of TMPyP4 (4 μM) and BRACO-19 (10 μM) in a model Mycobacterium smegmatis MC2155 strain. We found that 10% and 12% genes of the bacterium changed their expression under the action of TMPyP4 and BRACO-19, respectively. However, we found no statistically significant correlation between differential expression and the presence of PQS [9].

In this study, we aimed to assess the influence of subinhibitory concentrations of G4 ligands TMPyP4 (2 μM) and BRACO-19 (5 μM) on gene expression profiles in *M. smegmatis* MC^{2}155 and interprete the results in connection with the previously obtained data.

METHODS

Bacterial strain and cultivation conditions

In this study *Mycobacterium smegmatis* MC^{2}155 model strain was used in all experiments. The cultivation was carried out at 37 °C in a humid atmosphere containing 5% CO_2 using Middlebrook 7H9 broth (HiMedia; India) or Middlebrook 7H11 agar (HiMedia) with addition of 0.5% glycerol and 10% Middlebrook OADC growth supplement (HiMedia). Cryopreserved bacteria from a certified collection were seeded on agar plates and grown for 24 h before inoculation to a liquid medium.

Cultivation of *M. smegmatis* for the transcriptomic analysis was carried out in accordance with the previous publication [9]. Bacterial cells were grown to 0.47 optical density measured at 570 nm, corresponding to the mid-exponential phase, and transferred to 5 mL tubes (NUOVA APTACA; Italy). G4-stabilizing agents were added to the cultures in final concentrations corresponding to a half of minimal inhibitory concentration (5 μM for BRACO-19 and 2 μM for TMPyP4). The cells were incubated for 4 h (cell division time described previously [10]) at 37 °C in a humid atmosphere containing 5% CO_2 in a thermal shaker (250 rpm). All experiments were carried out in three biological replicates.

RNA extraction and transcriptomic analysis

RNA extraction and transcriptomic assay were carried out using previously described protocols [9]. Bacterial cells were

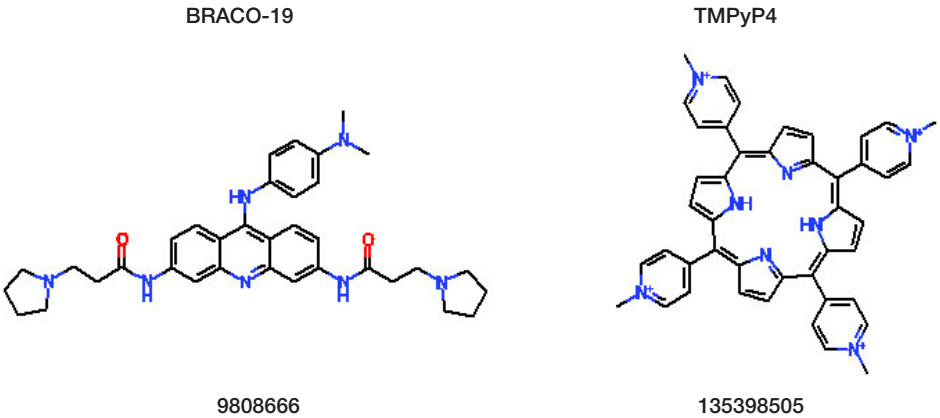

Fig. 1. Structural formulas of the BRACO-19 and TMPyP4 ligands

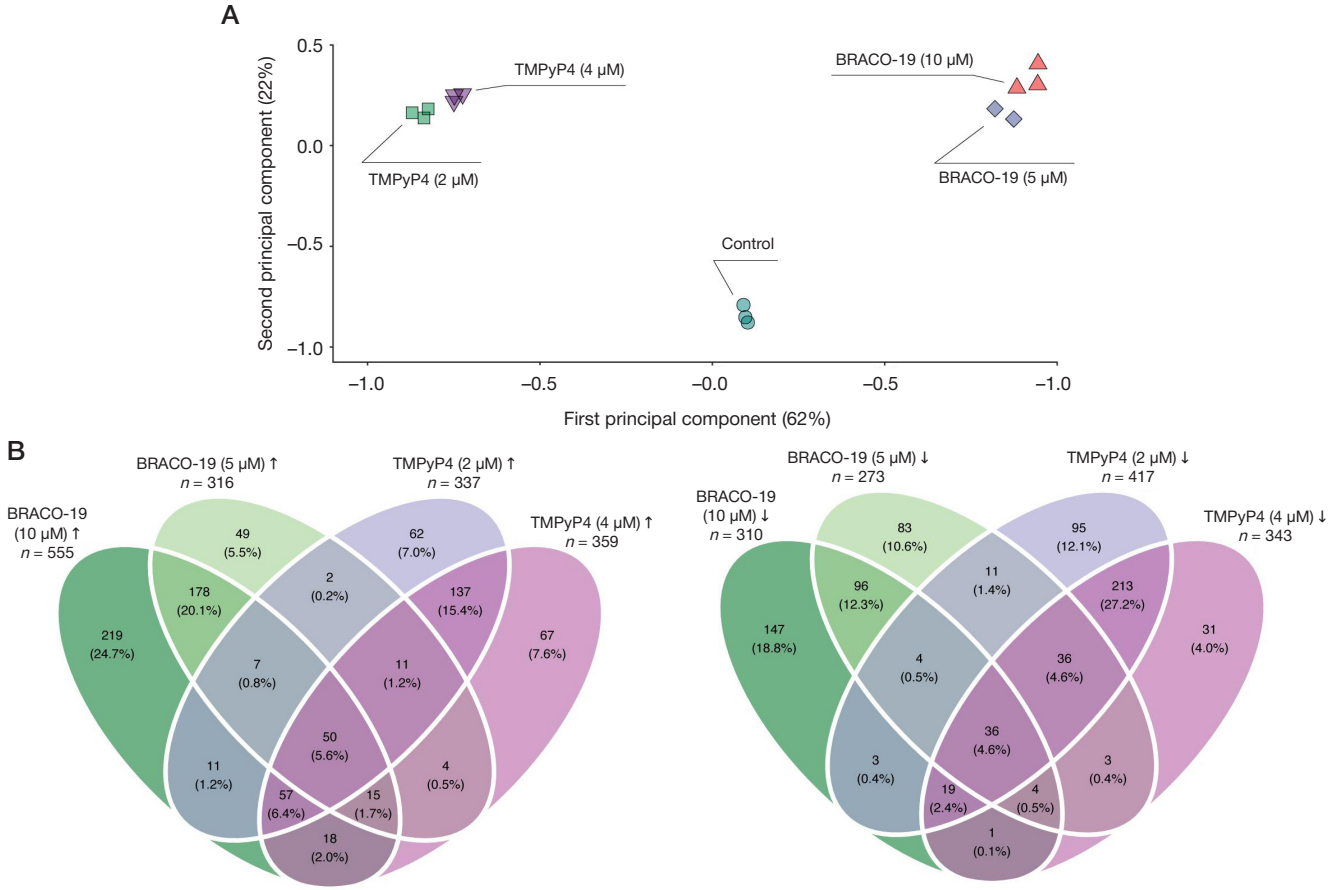

Fig. 2. Transcriptomic differences revealed in *Mycobacterium smegmatis* treated with different concentrations of BRACO-19 and TMPyP4. **A**. The principal components analysis shows correlations of gene expression levels under five sets of conditions (designated by *colors*). **B**. Venn diagrams show intersections among the sets of genes regulated by exposure to BRACO-19 and TMPyP4 in different concentrations

collected by centrifugation (8000 g, 10 min, 4 °C); the pellet was washed with phosphate buffered saline and mixed with RNAprotect Bacteria Reagent (Qiagen; USA) to stabilize RNA. The cells were lyzed in Lysing Matrix B 2 mL tubes placed in a MagNA Lyzer instrument (Roche; Switzerland) for 30 s. The lyzates were processed in a KingFisher automated station (Thermo Fisher Scientific; USA) using MagMAX mirVana Total RNA Isolation Kit (Thermo Fisher Scientific) in accordance with the manufacturer's protocol. The isolated total RNA was treated with TURBO DNA-free kit (Thermo Fisher Scientific) in a 50 μL volume. Additional RNA purification was performed with Agencourt RNA Clean XP kit (Beckman Coulter; USA).

The libraries were prepared starting from 300 ng of total RNA. The ribosomal RNA was removed by Ribo-Zero Plus rRNA Depletion Kit (Illumina; USA) in accordance with the manufacturer's protocol. The transcriptomic libraries were prepared using NEBNext Ultra II Directional RNA Library Prep Kit (NEB; USA). The libraries were pooled in equimolar amounts, diluted to a 12 pM final concentration and high-throughput sequenced on HiSeq 2500 Illumina platform using HiSeq Rapid SBS Kit v2 (50 cycles) and HiSeq SR Rapid Cluster Kit v2 with 1% Phix (Illumina) added as control. The sequencing data are deposited in NCBI (Accession: PRJNA765512).

Bioinformatics analysis

The sequencing reads were mapped to *M. smegmatis* MC²155 genome (CP000480.1) using HISAT2 [11]. The sorting of SAM files, their conversion to BAM files and subsequent indexing were carried out in SAMtools software [12]. The mapping quality and gene coverage were assessed using QualiMap [13]; the reports were aggregated by MultiQC [14]. The mapped reads were assigned to specific genes using featureCounts [15]. Differential gene expression analysis was performed with edgeR package [16] for R. Genes with false discovery rate (FDR) less than 0.05 and a fold change (log2FC) threshold of |1| (i.e. ≥ |2|-fold change) were considered differentially expressed. For intersample comparisons the counts were normalized using the gene length corrected trimmed mean of M-values [17]. Subsequent analysis of functional enrichment for GO terms (categories) and KEGG pathways involving differentially expressed genes was performed with clusterProfiler package [18]; the categories were considered enriched at FDR ≤ 0.05.

RESULTS

Transcriptomic influence of G4-stabilizing ligands BRACO-19 and TMPyP4 in *M. smegmatis* MC²155

To assess the influence of G4 ligands on transcriptomic profiles of *M. smegmatis*, the bacteria were exposed to subinhibitory concentrations of BRACO-19 and TMPyP4 (5 μM and 2 μM, respectively) for 4 h. The results of RNA sequencing for the ligand-treated bacterial cultures were compared mutually as well as against previously obtained data for higher, inhibitory concentrations of the ligands (10 μM and 4 μM, respectively).

The principal components analysis revealed clusterization of the replicates in every experiment as well as pronounced effects of both ligands compared with the control (Fig. 2A). At the same time, the analysis revealed close similarity of the effects for different concentrations of the same ligand.

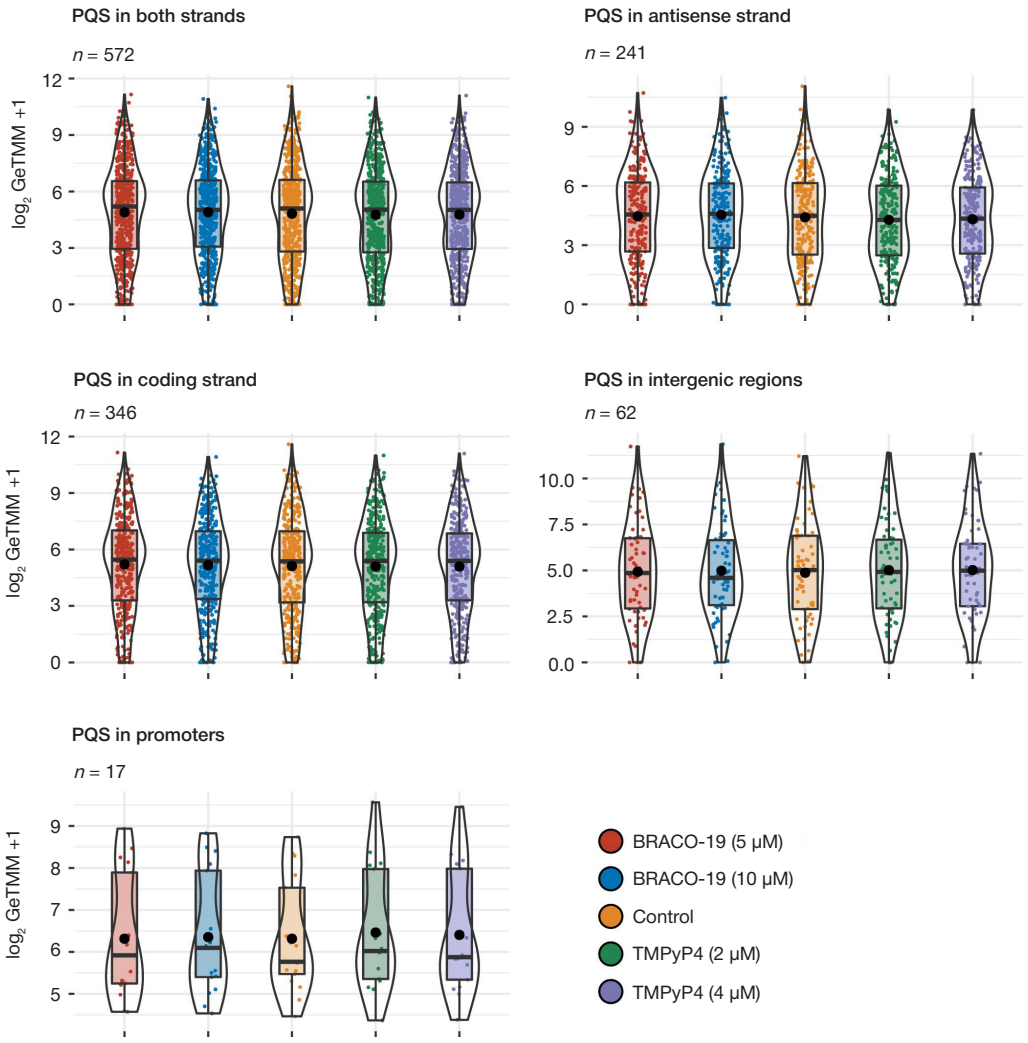

Fig. 3. Boxplot showing differential expression of PQS-containing genes in *Mycobacterium smegmatis* exposed to different concentrations of BRACO-19 and TMPyP4. The number of genes with PQS (n) excludes genes with low CPM (Counts Per Million); for PQS in intergenic regions, both flanking genes are included. Box limits correspond to lower and upper quartiles; horizontal line inside the box indicates the median and *black dot* indicates the mean value. Games-Howell post hoc test was applied to calculate *p* values

For BRACO-19, we identified 589 (316↑; 273↓) and 865 (555↑; 310↓) differentially expressed genes at 5 μM and 10 μM, respectively (Fig. 2B). For TMPyP4, we observed the opposite trend with decreased number of differentially expressed genes at higher concentration of the ligand: 754 (337↑; 417↓) and 702 (359↑; 343↓) for 2 μM and 4 μM, respectively.

Ligand-induced changes in expression of genes associated with putative quadruplex-forming sequences

Correlations of the ligand sensitivity with the presence of putative quadruplex-forming sequences were assessed for the following groups of genes identified previously: PQS in both DNA strands (615 genes of n = 665), PQS in coding strand (255 genes of n = 267), PQS in antisense (template) strand (360 genes of n = 398), PQS in intergenic regions (two flanking genes for 14 elements of n = 53) and PQS in promoter regions (17 genes of n = 17) [9]. Both ligands revealed no statistically significant differences with control samples for all groups of genes regardless of concentration (Games-Howell post-hoc test $p_{adj.} >> 0.05$; Fig. 3).

Interestingly, the number of differentially expressed quadruplex-associated genes increased as 58 → 75 with increasing concentration of BRACO-19 (5 μM → 10 μM), but decreased as 72 → 59 with increasing concentration of TMPyP4 (2 μM → 4 μM) (Fig. 4).

Ligand-induced changes in expression of genes of the replication and repair system

Comparative analysis of RNA sequencing data for BRACO-19 and TMPyP4 revealed their differential influence on the replication and repair system of *M. smegmatis* at transcriptional level (see Table). The effects of BRACO-19 included elevated expression levels for DNA gyrases, translesion synthesis DNA polymerases, DNA and RNA helicases and DNA repair system proteins. Translesion synthesis DNA polymerases are SOS response proteins involved in active recovery of the bacterial chromosome integrity [19]. DNA gyrases (type II topoisomerases) participate in DNA synthesis by introducing negative supercoils [20], whereas methyltransferase Ogt and DNA glycosylase AlkA prevent DNA damage during alkylation [21]. It should be noted that the use of BRACO-19 in subinhibitory concentration (5 μM) affected expression of fewer genes compared with the inhibitory concentration (10 μM). A > 2-fold increase in expression upon switching the dose of BRACO-19 from subinhibitory to inhibitory, observed for *ogt* and *alkA* genes only, may indicate a specific dose-dependent effect of the given ligand on these genes.

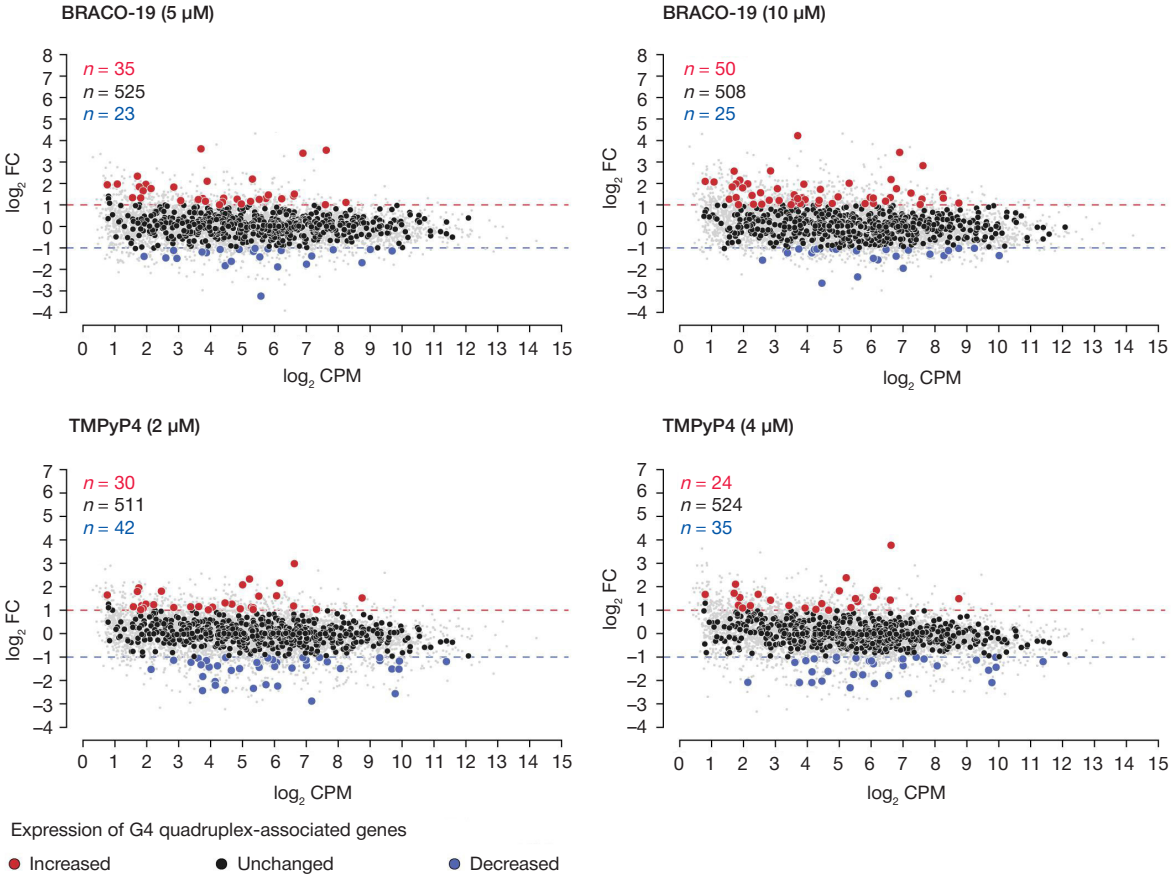

Fig. 4. Mean-difference plots (MD-plots) of fold changes (log_2 FC) versus average expression levels (log_2 CPM) for the putative quadruplex-associated genes

For TMPyP4, the only gene with an increased expression level of the repair system was *ssbb*. This gene encodes a protein which participates in replication and recombination repair processes through binding to single-stranded DNA to keep it from rehybridization. Expression level of the DNA helicase gene RecQ was increased by both ligands.

Ligand-induced changes in metabolic pathways of *M. smegmatis* MC²155

The analysis of GO terms and KEGG pathways revealed significant enrichments (FDR < 0.05; Fig. 5) for the transcription (GO:0006351), arginine biosynthesis (GO:0006526), transport (GO:0006810), sulfur metabolism (msm00920), siderophore group nonribosomal peptide biosynthesis (msm01053) and ABC transporter (msm02010) functionalities.

Similarly, with the use of BRACO-19 in inhibitory concentrations, the exposure to subinhibitory levels of the same compound affected the only metabolic pathway associated with iron metabolism. The analysis identified elevated expression of genes involved in siderophore biosynthesis, transport, and reuptake. By contrast, genes involved in iron storage showed reduced expression. It is important to note that, judging by the level of enrichment, the response of the bacterial cell to subinhibitory concentrations of the ligand was stronger.

The use of TMPyP4 stimulated expression of transcription factor-encoding genes (GO:0006351) and genes involved in sulfur metabolism (msm00920) associated with the enrichment of cellular transport systems observed at different concentrations of the ligand: the majority of GO:0006810, msm02010 and msm00920 genes were common between these groups. By contrast, genes involved in arginine biosynthesis (GO:0006526) showed reduced expression at both concentrations of the ligand.

DISCUSSION

This study continues our previous research on the transcriptomic response of *M. smegmatis* to inhibitory concentrations of G4-stabilizing compounds BRACO-19 and TMPyP4 [9]. In this work, we used subinhibitory concentrations of the ligands for more refined specification of the links between PQS and gene expression, as well as identification of primary responders among metabolic pathways.

The bioinformatics analysis revealed extensive transcriptomic alterations induced by subinhibitory concentrations of G4 ligands (Fig. 2). The influence of ligand concentration on the extent of transcriptomic effect depended on the ligand: increasing the ligand concentration to inhibitory led to either increase or decrease in the number of differentially expressed genes (for BRACO-19 and TMPyP4, respectively). Further analysis of the data revealed no significant regulation of PQS-associated genes by G4 ligands or concentration-dependent ligand-mediated G4 stabilization (Fig. 3). We also analyzed common effects of the two ligands by focusing on particular genes reacting similarly to both ligands by either up- or downregulation. However, even for genes selected on this basis, we failed to find specific evidence of the ligand-mediated G4 stabilization or dose-dependent effects. Stabilization of the quadruplex structures previously described in *M. tuberculosis* could not be confirmed, given significant genomic divergence between *M. tuberculosis* and *M. smegmatis*.

The analysis of KEGG pathways and GO categories also revealed no signs of dose dependency. All transcriptomic effects exerted by subinhibitory concentrations of the ligands were consistent with the previously published results obtained by using inhibitory concentrations of these ligands [9] (Fig. 5). The only interesting exception is transcriptomic representation

Table. Changes in the replication and repair system gene expression in *M. smegmatis* under the action of BRACO-19 and TMPyP4

Locus	Gene	Product	Expression levels under the action of BRACO-19 compared with the control		Expression levels under the action of TMPyP4 compared with the control	
			5 μM	10 μM	2 μM	4 μM
MSMEG_0005	*gyrB*	DNA gyrase subunit B	**2.485372***	**2.304708**	–1.79363	–1.70249
MSMEG_0006	*gyrA*	DNA gyrase subunit A	**2.152993**	**2.316561**	**–2.34404**	–1.84273
MSMEG_1327	*recB*	Exodeoxyribonuclease subunit B	1.158257	1.240121	–2.16073	–2.2508
MSMEG_1620	*imuA′*	Hypothetical protein	1.957144	**2.865713**	1.419836	–1.08999
MSMEG_1622	*imuB*	Repair DNA polymerase	1.867917	**2.435738**	1.721681	1.944552
MSMEG_1633	*dnaE2*	Translesion synthesis DNA polymerase	1.855874	**2.529669**	1.720836	1.865113
MSMEG_2442	*RNaseH2* (*rnhB*)	Ribonuclease HII	1.845015	**2.135989**	1.353681	1.362699
MSMEG_3172	*dinB1*	DNA polymerase IV	2.069791	**2.304246**	1.066778	1.130623
MSMEG_3885	*helY*	DEAD/DEAH family RNA helicase	2.540092	**3.424716**	–1.17839	–1.13342
MSMEG_4701	*ssbb*	Single-stranded DNA-binding protein	1.509562	1.910513	**2.236647**	**2.367929**
MSMEG_4925	*alkA*	Transcription regulator, Ada family protein/ DNA-3-methyladenine glycosylase II	**3.608202**	**8.892216**	1.477495	1.539172
MSMEG_4928	*ogt*	Cysteine methyltransferase	**4.145998**	**9.941453**	1.106208	1.357626
MSMEG_5397	*recQ*	ATP-dependent DNA helicase RecQ	**3.156958**	**4.455866**	**2.107502**	**2.911045**
MSMEG_5422	*mazG*	Pyrophosphohydrolase	1.754292	1.586085	**–2.46206**	**–2.19913**
MSMEG_6443	*dinB3*	DNA polymerase IV	**2.077001**	**2.867936**	1.164152	1.261415
MSMEG_6896	*ssba*	Single-stranded DNA-binding protein	–1.70995	**–2.71083**	–1.27025	–1.32274

Note: * — bold typed are entries complying with the following criteria: more than 2-fold change and FDR < 0.05.

of the iron metabolism system, which reacted to BRACO-1 with higher enrichment at subinhibitory concentrations of the ligand. This cellular system becomes activated under conditions of iron deficiency, with oxidative or nitrosative stress, as well as under increased demand for metalloproteins involved in DNA replication and repair [22]. The use of BRACO-19 in subinhibitory concentrations led to overrepresentation of the siderophore nonribosomal peptide biosynthesis pathway (msm01053) including the mycobactin synthesis genes. Other systems of the pathway revealed a gradual increase in gene expression levels at higher concentrations of the ligand.

Among the replication and repair system genes of *M. smegmatis*, the only gene activated by subinhibitory concentrations of BRACO-19 and TMPyP4 was *recQ*. The ability of RecQ helicase to resolve the quadruplex structures has been demonstrated for *E. coli*; however, RecQ of

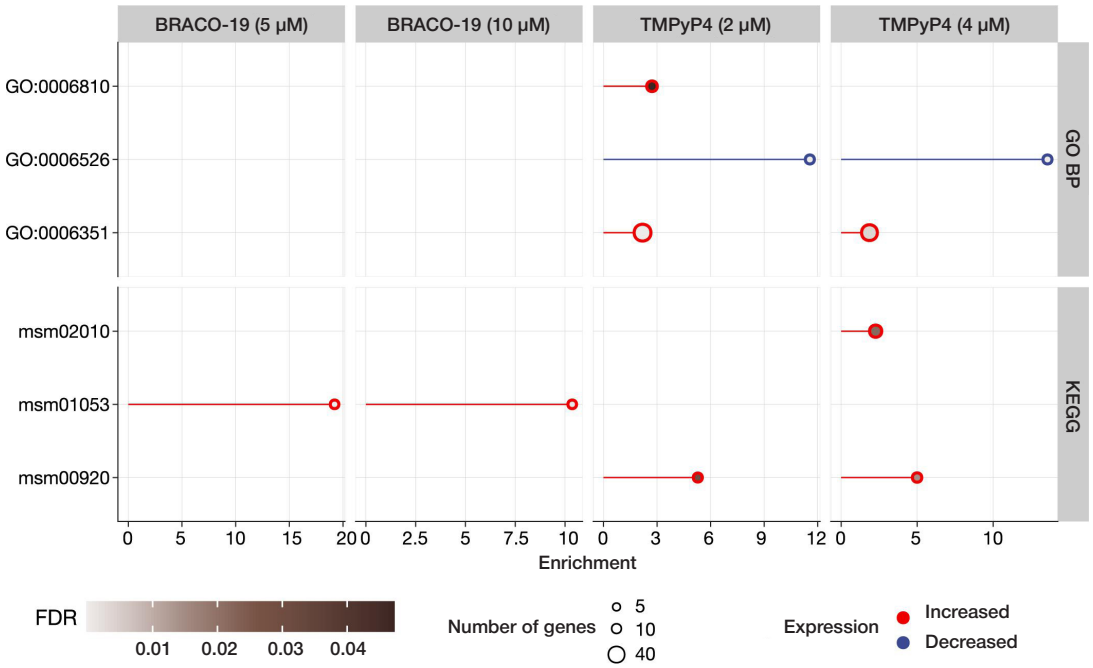

Fig. 5. GO categories and KEGG pathways showing enrichment under exposure to BRACO-19 and TMPyP4 in different concentrations: GO:0006810 — Transport; GO:0006526 — Arginine biosynthesis; GO:0006351 — DNA-dependent transcription; msm02010 — ABC transporters; msm01053 — Biosynthesis of siderophore group nonribosomal peptides; msm00920 — Sulfur metabolism

M. smegmatis is not homologous to the eponymous protein of *E. coli*; moreover, RecQ is absent in *M. tuberculosis* [23]. This point questions the ability of RecQ protein of *M. smegmatis* to resolve G4 structures and subjects it to further scrutiny.

It should be recognized that transcriptional response in bacteria is a complex phenomenon modulated by multiple factors, including subtle genetic differences, environmental exposures, etc. Recent findings indicate that quadruplexes, apart from their inhibitory effect, can act as transcriptional activators depending on the conditions. In eukaryotes, quadruplexes may provide structural cores for transcription factor binding and promote functional changes in chromatin architecture, R-loop stabilization, etc. [24]. In bacteria, the quadruplex stabilization by naphthalene diimide derivatives has been shown to inhibit gene expression in Gram-negative strains while enhancing it in Gram-positive strains, which supports the bidirectional nature of the quadruplex-mediated regulation [25]. The regulatory role of RNA quadruplexes in bacteria should not be ignored, as their functional presence in prokaryotes has been proved experimentally [26]. The use of advanced techniques for quadruplex detection and verification, including proteomic experiments, will ensure further progress in our understanding of the role of particular G4 elements in genomic regulation.

CONCLUSIONS

Guanine quadruplexes, described in the majority of microorganisms, represent an important element of functional genomic regulation. The current study, however, secures no direct relationship between stabilization of the putative quadruplex structures and expression of genes associated with these structures. Both quadruplex-stabilizing ligands tested in this study exerted diverse transcriptomic effects, encompassing numerous genes and several metabolic pathways. The changes observed for the transcription factor-encoding genes and the replication and repair system genes under the action of these ligands indicate their potential involvement at the RNA/DNA level, consistently with the current concept of quadruplex-mediated genomic regulation. The enhanced transcription of RecQ DNA helicase gene observed in the studied systems positions its product as a plausible candidate enzyme participating in the resolution of quadruplex structures.

References

1. Global Tuberculosis Report 2021 [cited 2022 Apr 7]. Available from: https://www.who.int/teams/global-tuberculosis-programme/tb-reports/global-tuberculosis-report-2021.
2. Kadura S, King N, Nakhoul M, Zhu H, Theron G, Köser CU, et al. Systematic review of mutations associated with resistance to the new and repurposed Mycobacterium tuberculosis drugs bedaquiline, clofazimine, linezolid, delamanid and pretomanid. Journal of Antimicrobial Chemotherapy. 2020; 75 (8): 2031.
3. Spiegel J, Adhikari S, Balasubramanian S. The structure and function of DNA G-quadruplexes. Trends Chem. 2020; 2 (2): 123–36.
4. Masai H, Tanaka T. G-quadruplex DNA and RNA: Their roles in regulation of DNA replication and other biological functions. Biochemical and Biophysical Research Communications. 2020; 531 (1): 25–38.
5. Bartas M, Cutová M, Brázda V, Kaura P, Šťastný J, Kolomazník J, et al. The presence and localization of G-quadruplex forming sequences in the domain of bacteria. Molecules. 2019; 24 (9).
6. Yadav P, Kim N, Kumari M, Verma S, Sharma TK, Yadav V, et al. G-quadruplex structures in bacteria: biological relevance and potential as an antimicrobial target. Journal of Bacteriology. 2021; 203 (13).
7. Perrone R, Lavezzo E, Riello E, Manganelli R, Palù G, Toppo S, et al. Mapping and characterization of G-quadruplexes in Mycobacterium tuberculosis gene promoter regions. Sci Rep. 2017; 7 (1).
8. Mishra SK, Shankar U, Jain N, Sikri K, Tyagi JS, Sharma TK, et al. Characterization of G-quadruplex motifs in espB, espK, and cyp51 genes of mycobacterium tuberculosis aspotential drug targets. Mol Ther Nucleic Acids. 2019; 16: 698–706.
9. Shitikov E, Bespiatykh D, Malakhova M, Bespyatykh J, Bodoev I, Vedekhina T, et al. Genome-wide tanscriptional response of mycobacterium smegmatis MC 2 155 to G-quadruplex ligands BRACO-19 and TMPyP4. Front Microbiol. 2022; 13.
10. Logsdon MM, Aldridge BB. Stable regulation of cell cycle events in mycobacteria: insights from Inherently heterogeneous bacterial populations. Front Microbiol. 2018; 9 (MAR).
11. Kim D, Langmead B, Salzberg SL. HISAT: a fast spliced aligner with low memory requirements. Nat Methods. 2015; 12 (4): 357–60.
12. Li H, Handsaker B, Wysoker A, Fennell T, Ruan J, Homer N, et al. The sequence alignment/map format and SAMtools. Bioinformatics. 2009; 25 (16): 2078–9.
13. Okonechnikov K, Conesa A, García-Alcalde F. Qualimap 2: advanced multi-sample quality control for high-throughput sequencing data. Bioinformatics. 2016; 32 (2): 292–4.
14. Ewels P, Magnusson M, Lundin S, Käller M. MultiQC: summarize analysis results for multiple tools and samples in a single report. Bioinformatics. 2016; 32 (19): 3047–8.
15. Liao Y, Smyth GK, Shi W. featureCounts: an efficient general purpose program for assigning sequence reads to genomic features. Bioinformatics. 2014; 30 (7): 923–30.
16. Robinson MD, McCarthy DJ, Smyth GK. edgeR: a Bioconductor package for differential expression analysis of digital gene expression data. Bioinformatics. 2010; 26 (1): 139–40.
17. Smid M, Coebergh van den Braak RRJ, van de Werken HJG, van Riet J, van Galen A, de Weerd V, et al. Gene length corrected trimmed mean of M-values (GeTMM) processing of RNA-seq data performs similarly in intersample analyses while improving intrasample comparisons. BMC Bioinformatics. 2018; 19 (1).
18. Yu G, Wang LG, Han Y, He QY. clusterProfiler: an R package for comparing biological themes among gene clusters. OMICS. 2012; 16 (5): 284–7.
19. W Yang, Y Gao. Translesion and repair DNA polymerases: diverse structure and mechanism. Annu Rev Biochem. 2018; 87: 239–61.
20. Mdluli K, Ma Z. Mycobacterium tuberculosis DNA gyrase as a target for drug discovery. Infect Disord Drug Targets. 2007; 7 (2): 159–68.
21. Yang M, Aamodt RM, Dalhus B, Balasingham S, Helle I, Andersen P, et al. The ada operon of Mycobacterium tuberculosis encodes two DNA methyltransferases for inducible repair of DNA alkylation damage. DNA Repair. 2011; 10 (6): 595–602.
22. Namouchi A, Gómez-Muñoz M, Frye SA, Moen LV, Rognes T, Tønjum T, et al. The Mycobacterium tuberculosis transcriptional landscape under genotoxic stress. BMC Genomics. 2016; 17 (1): 1–13.
23. Wu X, Maizels N. Substrate-specific inhibition of RecQ helicase. Nucleic Acids Research. 2001; 29 (8): 1765–71.
24. Robinson J, Raguseo F, Nuccio SP, Liano D, di Antonio M. DNA G-quadruplex structures: more than simple roadblocks to transcription? Nucleic Acids Res. 2021; 49 (15): 8419–31.
25. Cebrián R, Belmonte-Reche E, Pirota V, de Jong A, Morales JC, Freccero M, et al. G-quadruplex DNA as a target in pathogenic bacteria: efficacy of an extended naphthalene diimide ligand and Its mode of action. Journal of Medicinal Chemistry. 2021.
26. Shao X, Zhang W, Umar MI, Wong HY, Seng Z, Xie Y, et al. RNA G-quadruplex structures mediate gene regulation in bacteria. mBio. 2020; 11 (1).

Литература

1. Global Tuberculosis Report 2021 [cited 2022 Apr 7]. Available from: https://www.who.int/teams/global-tuberculosis-programme/tb-reports/global-tuberculosis-report-2021.
2. Kadura S, King N, Nakhoul M, Zhu H, Theron G, Köser CU, et al. Systematic review of mutations associated with resistance to the new and repurposed Mycobacterium tuberculosis drugs bedaquiline, clofazimine, linezolid, delamanid and pretomanid. Journal of Antimicrobial Chemotherapy. 2020; 75 (8): 2031.
3. Spiegel J, Adhikari S, Balasubramanian S. The structure and function of DNA G-quadruplexes. Trends Chem. 2020; 2 (2): 123–36.
4. Masai H, Tanaka T. G-quadruplex DNA and RNA: Their roles in regulation of DNA replication and other biological functions. Biochemical and Biophysical Research Communications. 2020; 531 (1): 25–38.
5. Bartas M, Cutová M, Brázda V, Kaura P, Šťastný J, Kolomazník J, et al. The presence and localization of G-quadruplex forming sequences in the domain of bacteria. Molecules. 2019; 24 (9).
6. Yadav P, Kim N, Kumari M, Verma S, Sharma TK, Yadav V, et al. G-quadruplex structures in bacteria: biological relevance and potential as an antimicrobial target. Journal of Bacteriology. 2021; 203 (13).
7. Perrone R, Lavezzo E, Riello E, Manganelli R, Palù G, Toppo S, et al. Mapping and characterization of G-quadruplexes in Mycobacterium tuberculosis gene promoter regions. Sci Rep. 2017; 7 (1).
8. Mishra SK, Shankar U, Jain N, Sikri K, Tyagi JS, Sharma TK, et al. Characterization of G-quadruplex motifs in espB, espK, and cyp51 genes of mycobacterium tuberculosis aspotential drug targets. Mol Ther Nucleic Acids. 2019; 16: 698–706.
9. Shitikov E, Bespiatykh D, Malakhova M, Bespyatykh J, Bodoev I, Vedekhina T, et al. Genome-wide tanscriptional response of mycobacterium smegmatis MC 2 155 to G-quadruplex ligands BRACO-19 and TMPyP4. Front Microbiol. 2022; 13.
10. Logsdon MM, Aldridge BB. Stable regulation of cell cycle events in mycobacteria: insights from Inherently heterogeneous bacterial populations. Front Microbiol. 2018; 9 (MAR).
11. Kim D, Langmead B, Salzberg SL. HISAT: a fast spliced aligner with low memory requirements. Nat Methods. 2015; 12 (4): 357–60.
12. Li H, Handsaker B, Wysoker A, Fennell T, Ruan J, Homer N, et al. The sequence alignment/map format and SAMtools. Bioinformatics. 2009; 25 (16): 2078–9.
13. Okonechnikov K, Conesa A, García-Alcalde F. Qualimap 2: advanced multi-sample quality control for high-throughput sequencing data. Bioinformatics. 2016; 32 (2): 292–4.
14. Ewels P, Magnusson M, Lundin S, Käller M. MultiQC: summarize analysis results for multiple tools and samples in a single report. Bioinformatics. 2016; 32 (19): 3047–8.
15. Liao Y, Smyth GK, Shi W. featureCounts: an efficient general purpose program for assigning sequence reads to genomic features. Bioinformatics. 2014; 30 (7): 923–30.
16. Robinson MD, McCarthy DJ, Smyth GK. edgeR: a Bioconductor package for differential expression analysis of digital gene expression data. Bioinformatics. 2010; 26 (1): 139–40.
17. Smid M, Coebergh van den Braak RRJ, van de Werken HJG, van Riet J, van Galen A, de Weerd V, et al. Gene length corrected trimmed mean of M-values (GeTMM) processing of RNA-seq data performs similarly in intersample analyses while improving intrasample comparisons. BMC Bioinformatics. 2018; 19 (1).
18. Yu G, Wang LG, Han Y, He QY. clusterProfiler: an R package for comparing biological themes among gene clusters. OMICS. 2012; 16 (5): 284–7.
19. W Yang, Y Gao. Translesion and repair DNA polymerases: diverse structure and mechanism. Annu Rev Biochem. 2018; 87: 239–61.
20. Mdluli K, Ma Z. Mycobacterium tuberculosis DNA gyrase as a target for drug discovery. Infect Disord Drug Targets. 2007; 7 (2): 159–68.
21. Yang M, Aamodt RM, Dalhus B, Balasingham S, Helle I, Andersen P, et al. The ada operon of Mycobacterium tuberculosis encodes two DNA methyltransferases for inducible repair of DNA alkylation damage. DNA Repair. 2011; 10 (6): 595–602.
22. Namouchi A, Gómez-Muñoz M, Frye SA, Moen LV, Rognes T, Tønjum T, et al. The Mycobacterium tuberculosis transcriptional landscape under genotoxic stress. BMC Genomics. 2016; 17 (1): 1–13.
23. Wu X, Maizels N. Substrate-specific inhibition of RecQ helicase. Nucleic Acids Research. 2001; 29 (8): 1765–71.
24. Robinson J, Raguseo F, Nuccio SP, Liano D, di Antonio M. DNA G-quadruplex structures: more than simple roadblocks to transcription? Nucleic Acids Res. 2021; 49 (15): 8419–31.
25. Cebrián R, Belmonte-Reche E, Pirota V, de Jong A, Morales JC, Freccero M, et al. G-quadruplex DNA as a target in pathogenic bacteria: efficacy of an extended naphthalene diimide ligand and Its mode of action. Journal of Medicinal Chemistry. 2021.
26. Shao X, Zhang W, Umar MI, Wong HY, Seng Z, Xie Y, et al. RNA G-quadruplex structures mediate gene regulation in bacteria. mBio. 2020; 11 (1).